Hindawi Publishing Corporation
Advances in Materials Science and Engineering
Volume 2014, Article ID 476079, 6 pages
http://dx.doi.org/10.1155/2014/476079

Research Article

Reactivity and Microstructure of Al_2O_3-Reinforced Magnesium-Matrix Composites

Maher Mounib,[1] Matteo Pavese,[2] Claudio Badini,[2] Williams Lefebvre,[1] and Hajo Dieringa[3]

[1] *Groupe de Physique des Matériaux (GPM), Avenue de L'Université, B.P. 12, 76801 Saint Étienne du Rouvray, France*
[2] *Politecnico di Torino, Corso Duca degli Abruzzi 24, 10129 Torino, Italy*
[3] *Helmholtz-Zentrum Geesthacht, Zentrum für Material- und Küstenforschung GmbH, Max-Planck-Straße, 21502 Geesthacht, Germany*

Correspondence should be addressed to Maher Mounib; maher.mounib@gmail.com

Received 20 June 2014; Accepted 10 August 2014; Published 10 September 2014

Academic Editor: Kamineni Pitcheswara Rao

Performances of metal matrix composites (MMCs) rely strongly on the distribution of particles within the metal matrix but also on the chemical reaction which may occur at the liquid-solid interfaces. This paper presents the chemical reaction between aluminum based particles Al_2O_3 and Al_2O_3-AlOOH with magnesium alloys matrixes AZ91 and EL21, respectively, and studies the microstructure of these reinforced composites. Different methods such as transmission electron microscopy (TEM), differential scanning calorimetry (DSC), and XRD were used to highlight these chemical reactions and to identify products. Results demonstrate the formation of MgO particles within the matrix for both composites and also the dissolution of aluminum in the eutectic region in the case of EL21.

1. Introduction

Metal matrix composites have been catching industrials' attention due to their mechanical properties. Their potential importance has increased in a variety of fields such as aerospace and automotive industries where the increasing fuel price is leading to the necessity to overcome the weight reduction issue, but they also find applications in electronic industries. Due to their low density, aluminum and magnesium alloys are very interesting as matrix in MMCs. Through the addition of submicron-sized particles it is possible to achieve an enhancement of properties with respect to base alloys, such as the yield strength, ultimate tensile strength, hardness, and stiffness. Based on total strengthening effect models [1] it is suggested that MMCs can be effectively strengthened by the use of small particles closely spaced together.

There are various processing methods to elaborate MMCs such as liquid state processing, spray deposition techniques, and solid state processing routes. Each process has its own advantages, drawbacks, and applications. Besides, the processing route impacts directly on the mechanical properties and microstructures of these composites [2]. Among these processes used to produce metal matrix composites, stir casting is widely used because this processing method is flexible and economically viable and allows mass production. In this process reinforcement particles are incorporated into the molten alloy, while a continuous mixing is set to obtain a suitable dispersion and then the solidification of the molten alloy occurs under specific conditions to obtain the desired distribution. Despite the convenience of the process, liquid stirring has also some major problems [3, 4] such as the poor wetting of the reinforcement particles by the liquid metal matrix and the tendency of reinforcement particles to sink or float depending on their density relative to that of the melt. In addition, there is the tendency of particles to agglomerate and form large clusters, an effect that increases significantly when the size of the reinforcement decreases. By coupling external fields such as electromagnetic field, power ultrasound, or high-energy liquid shearing to liquid metal processing, it

Table 1: Chemical composition (in wt.%) of AZ91 Mg-alloy.

Al	Zn	Mn	Si	Fe	Cu	Ni	Mg
8.71	0.66	0.22	0.043	0.001	0.002	0.001	Bal.

Table 2: Chemical composition (in wt.%) of EL21 Mg-alloy.

Nd	Gd	Zn	Zr	Mg
2.6–3.1	1.0–1.7	0.2–0.5	Saturated	Bal.

seems possible to overcome these issues, by improving the dispersion of particles to obtain a homogeneous distribution into the melt and in the mold after the solidification step.

In the last years, many papers have been published on magnesium-matrix composites containing aluminum oxide particles, demonstrating some interesting properties of these composites regarding mechanical properties [5–10], oxidation resistance [11], and wear behavior [12, 13]. However most of these studies neglect the possible chemical interaction between matrix and reinforcement, even if this phenomenon is well known from past studies on magnesium-matrix composites [14–16].

The aim of this work is to study the chemical interaction between aluminum oxide-based particles and the magnesium alloy matrix and to characterize the microstructure of AZ91 and EL21 alloys reinforced with such particles.

2. Materials and Methods

Materials were produced at the Helmholtz Zentrum Geesthacht (HZG), Germany. Chemical compositions of the AZ91 and Elektron 21 (EL21) Mg-alloy are listed in Tables 1 and 2, respectively. Al_2O_3 and Al_2O_3-AlOOH ceramic particles with an average size of 250 nm and 0.5–1 μm, respectively, were used as the reinforcing materials for AZ91 and EL21, respectively. A liquid stirring process coupled with an ultrasonic external field has been used to produce these composites. Ceramic particles (1 wt.%) were introduced into the molten alloy; the homogenization of the mixture was conducted first using high speed stirring (200 rpm); then a power ultrasound external field was applied with the aim of obtaining a homogeneous distribution; then the metal was cooled down by water quenching. In this process the particles are in contact with the melt between seven and eight minutes.

Microstructural characterization of both composites was carried out by transmission electron microscopy (TEM). The microscope was a JEOL JEM 2010 operating at 200 kV and equipped with a LaB_6 filament. The incertitude of the EDS results obtained using this TEM is ±1%. Samples were prepared from 3 mm diameter disks (average thickness of 150 μm) followed by mechanical grinding with a dimple and finally by ion milling at room temperature (final energy of Ar ions set to 1.5 keV).

DSC reaction studies were carried out on a Perkin Elmer Pyris DSC 7 instrument, from room temperature at 700°C at the heating rate of 20°C/min in a flowing argon atmosphere. Steel crucibles were used to minimize the thermal effects linked to possible reactions between the magnesium alloy and the crucibles. The reaction was studied by mixing overnight powders of the metal and of the ceramic in a volume ratio 1 : 1 and then by cold pressing the powder mixture into a 3 mm diameter disc that was then analyzed with the DSC. All the operations concerning magnesium powders were carried out into a glove box, in order to minimize the oxidation of the magnesium.

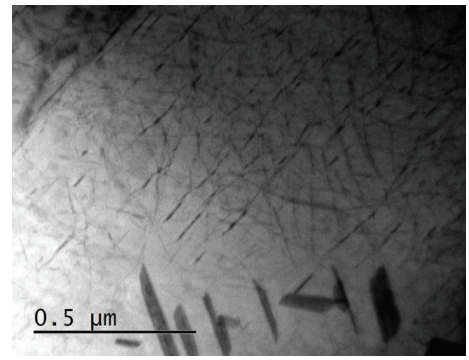

Figure 1: TEM BF picture of the microstructure of EL21 + Al_2O_3-AlOOH.

X-ray diffraction (XRD) was also carried out to characterize both the starting powders and the product of the reactions after the DSC runs. A Panalytical X'Pert Pro MPD instrument was used, with CuKα radiation. Both aluminum oxide powders resulted in a mixture of several polymorphs, mainly α, δ, and γ, but no other phases were observed.

3. Results and Discussion

Figure 1 shows a bright field (BF) TEM picture of the typical microstructure of EL21. After casting, the material displays a complex microstructure composed of a high number density of rare earth containing precipitates well distributed in the Mg crystals, which contribute to the good mechanical properties of this commercial alloy. The larger precipitates are observed in the vicinity of macrosegregation areas inherited by the solidification path. It must be pointed out that, in the EL21 + Al_2O_3-AlOOH composite, particles could not be found neither in the alloy matrix nor in the eutectic region. However, a significant amount of aluminum was identified in the eutectic region. This is illustrated by Figure 2, which shows EDS analyses supporting the preferential location of Al in the rare-earth rich phase formed during the eutectic solidification of the composite.

The detection of Al in the eutectic region does not however allow determining whether the Al detected comes from AlOOH or Al_2O_3. Nevertheless, the fact that strictly no Al_2O_3 particle could be detected neither in the matrix nor in the eutectic region suggests that Al detected in the eutectic region can come from both Al_2O_3 and AlOOH.

The absence of aluminum oxide particles coupled with the presence of elemental aluminum in the eutectic zone suggests that during the process aluminum oxide particles were not dissolved, but they underwent chemical reaction

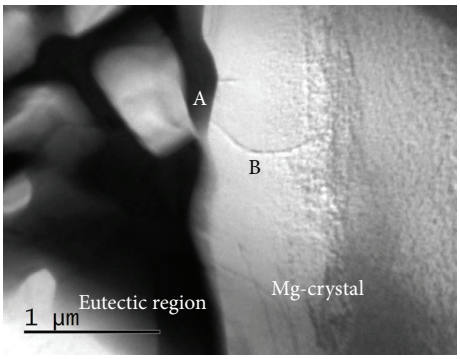

(a)

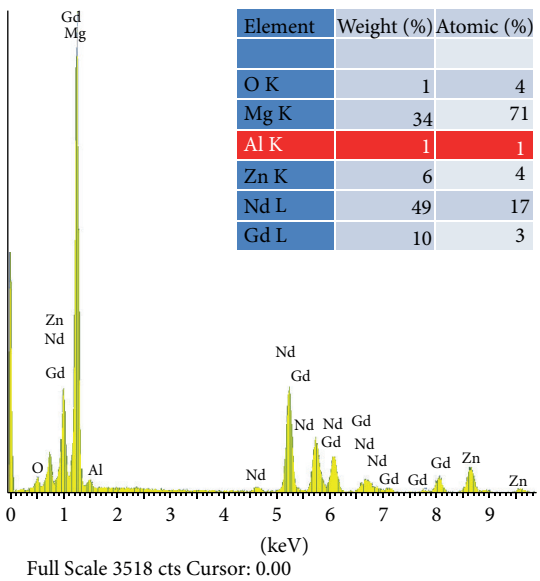

Element	Weight (%)	Atomic (%)
O K	1	4
Mg K	34	71
Al K	1	1
Zn K	6	4
Nd L	49	17
Gd L	10	3

(A)

Element	Weight (%)	Atomic (%)
O K	1	1
Mg K	95	98
Nd L	2	≈0
Gd L	2	≈0
Totals	100	

(B)

(b)

Figure 2: (a) BF TEM picture of a eutectic region of EL21 + Al_2O_3-AlOOH composite; (b) EDS spectra of the A and B areas.

with magnesium to form MgO, as confirmed by the direct TEM observation of MgO particles, as shown in Figure 3.

To better investigate the interaction between aluminum oxide particles and magnesium alloys, first thermodynamical calculation was performed. According to free Gibbs energies, the formation of MgO and $MgAl_2O_4$ is thermodynamically favorable as shown in the following reactions [17]:

$$\begin{gathered} Mg_{(l)} + Al_2O_{3(s)} = 3MgO_{(s)} + 2Al, \\ \Delta G_{(900^\circ C)} = -123\,\text{kJ/mol}, \end{gathered} \tag{1}$$

$$\begin{gathered} 3Mg_{(l)} + 4Al_2O_{3(s)} = 3MgAl_2O_{4(s)} + 2Al, \\ \Delta G_{(900^\circ C)} = -256\,\text{kJ/mol}. \end{gathered} \tag{2}$$

During the process, the melt is covered with the Ar/SF6 cover gas mixture and it is poured into the cylindric molds afterwards. During this pouring process the formation of MgO from the raw material is possible.

It is evident that the thermodynamics suggests that Al_2O_3 is not stable in magnesium and that, given a fixed quantity of aluminum oxide, the most probable phase formed by the reaction with magnesium is MgO.

In order to verify if the kinetics of these reactions is sufficient to guarantee the transformation of aluminum oxide into magnesium oxide, DSC measurements were carried out first on mixtures of pure magnesium and alumina and then on the mixtures of AZ91 or EL21 alloys with alumina. The results for pure Mg and EL21 alloy are shown in Figure 4.

From the DSC, it is evident that a strong reaction always occurs (the intense exothermic, down-heading peak), but the specific pathway of the reaction seems to change from the pure Mg case to the EL21 one. In the case of pure magnesium, an endothermic peak is observed at lower temperatures, corresponding to the Al-Mg eutectic melting. The reason for this different behavior is due to the fact that EL21 powders are rather coarse, while Mg ones are much finer. By changing the specific surface of the two powders, the contact surface between alloy and aluminum oxide changes, so that in the pure Mg case a significant interfacial reaction occurs before the main reaction peak. This reaction brings the formation of Al that dissolves in the Mg-alloy forming a Mg-Al alloy that melts at much lower temperature than pure Mg. Due to the low temperature, the interfacial Mg-Al_2O_3 reaction is relatively slow, so that the endothermic effect of the eutectic melting prevails on the exothermic effect of the reaction, and only an up-heading broad peak is observed. At higher temperature, the liquid Mg-Al alloy reacts strongly with the Al_2O_3 particles, causing the strong exothermic peak observed at 520°C.

In the case of EL21 alloy, the interfacial reaction is very small, due to the large size of Mg-alloy particles, and no evident thermal effect is observed. Only when the kinetics of the reaction is sufficiently fast, the reaction starts, and this brings a strong exothermic peak at 615°C that is so intense that covers also the endothermic melting peak of the Mg alloy.

The product of the reaction between Mg and Al_2O_3 was analyzed by XRD, as shown in Figure 5 for the case of pure magnesium.

From the XRD analysis it is possible to observe the phases Mg, MgO, γ-Al_2O_3, and $Al_{12}Mg_{17}$. The formation of MgO is evident, and the aluminum oxide residuum must not deceive. In this case, to maximize the thermal signal of the DSC, the reactants (Mg and aluminum oxide) are mixed

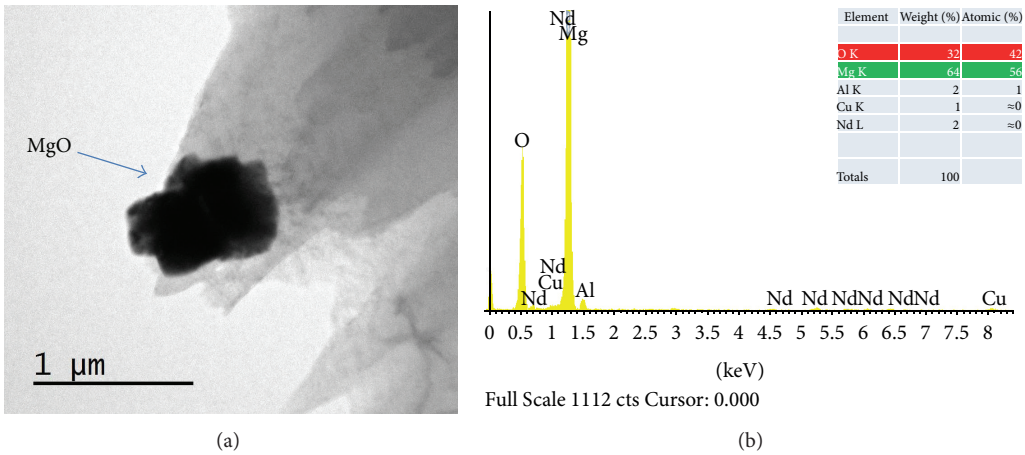

Figure 3: (a) BF TEM of MgO particle in EL21 + Al_2O_3-AlOOH composite; (b) EDS spectrum of MgO particle.

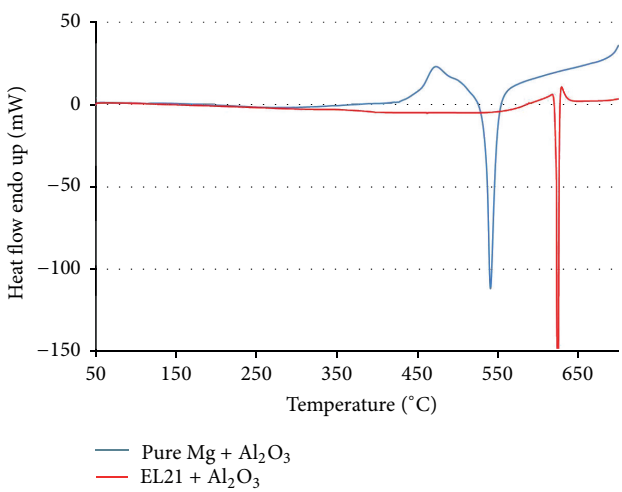

Figure 4: DSC of the reaction of pure Mg (blue) and Elektron 21 (red) with Al_2O_3.

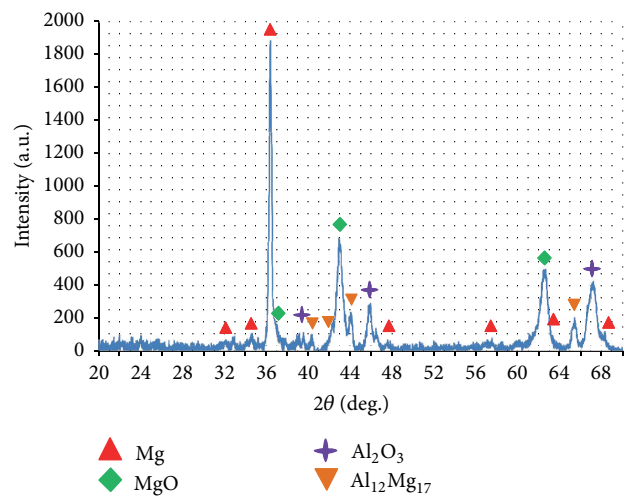

Figure 5: XRD of the product of the reaction between pure Mg and Al_2O_3.

in a 1:1 volume ratio, so that there is a very high quantity of aluminum oxide that cannot be completely consumed by magnesium. Thus it is not surprising that aluminum oxide is still present, and it is evident that MgO is formed and Al is dissolved in the Mg alloy, as confirmed by the formation of the $Al_{12}Mg_{17}$ phase.

Thus, the DSC and XRD analysis confirms that the reaction course for this composite material is correctly described by (1). MgO is more thermodynamically stable compared to Al_2O_3; therefore Mg tends to reduce Al_2O_3 in order to form MgO. The absence of $MgAl_2O_4$, less thermodynamically stable than MgO, is confirmed by the fact that no $MgAl_2O_4$ peak is observed on the XRD spectrum.

McLeod and Gabryel have studied the thermodynamic stability of several oxides with different magnesium concentrations [18]. At higher temperature and at very low Mg concentration $MgAl_2O_4$ spinel will be formed, while MgO is formed at lower temperature and higher Mg content. In the conditions of this work MgO is more stable.

The investigations of the AZ91 + Al_2O_3 lead to similar results. Whereas no alumina particle could be revealed in the Mg-matrix, MgO was observed. Also in this case, Al_2O_3 particles are hence proved to react in the melt, therefore leading to the formation of MgO which is shown in Figure 6 and confirmed with EDS results.

Our investigation demonstrates that incorporation of aluminum oxide particles in a molten Mg-based alloy leads to a systematic reaction of particles with the melt. For the EL21 alloy, the particle dissolution induces the segregation of Al to the eutectic region. On the opposite side, oxygen released by the reaction forms MgO particles inside the Mg-matrix. Moreover, the MgO particles identified in the TEM were systematically shown to range between several hundreds of nanometer and 1 μm. It is hence expected that, by tuning the cooling time, the size, and dispersion of

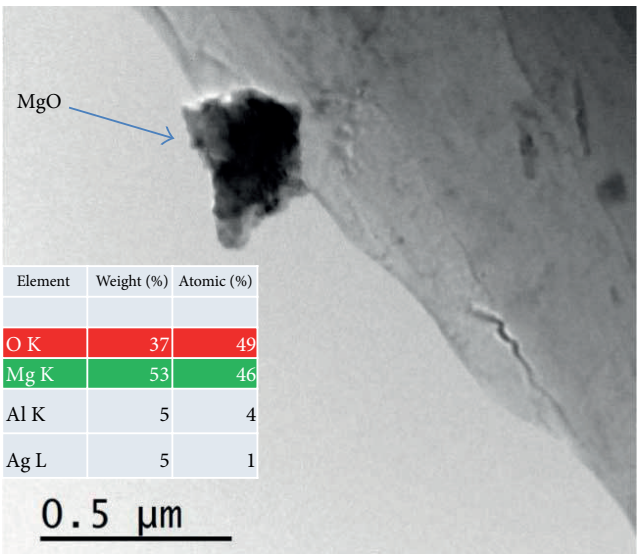

Figure 6: BF TEM of MgO particle in AZ91 + Al_2O_3 composite.

incorporated aluminum oxide particles, in situ formation of MgO might be further controlled and could lead to an interesting combination of microstructure and properties.

4. Conclusion

The behavior of Al_2O_3 and Al_2O_3-AlOOH ceramic particles after incorporation in molten magnesium alloys has been investigated. Rapid reaction of those particles with the melt occurred, as expected from thermodynamics and evidenced by DSC analyses, with formation of MgO and dissolution of Al in the melt. Aluminum was shown to be retained in the eutectic region in the case of the EL21 matrix composite. Meanwhile, it is demonstrated that incorporation in this process of Al_2O_3 and Al_2O_3-AlOOH to the molten Mg-based alloys investigated leads systematically to an interesting in situ formation of submicron scale MgO particles, which are significantly more stable in magnesium matrix than in alumina. This large stability is expected to increase the wetting of particles by the matrix and will reduce the pushing effect and therefore will avoid the agglomeration of particles. This chemical aspect could be used for in situ MMNCs processing.

Conflict of Interests

The authors declare that there is no conflict of interests regarding the publication of this paper.

Acknowledgment

The research leading to these results has been carried out under ExoMet project under the European Community's Seventh Framework Programme, Contract no. FP7-NMP3-LA-2012-280421.

References

[1] Z. Zhang and D. L. Chen, "Consideration of Orowan strengthening effect in particulate-reinforced metal matrix nanocomposites: a model for predicting their yield strength," *Scripta Materialia*, vol. 54, no. 7, pp. 1321–1326, 2006.

[2] J. Hashim, L. Looney, and M. S. J. Hashmi, "Metal matrix composites: production by the stir casting method," *Journal of Materials Processing Technology*, vol. 92-93, pp. 1–7, 1999.

[3] S. A. Sajjadi, H. R. Ezatpour, and M. Torabi Parizi, "Comparison of microstructure and mechanical properties of A356 aluminum alloy/Al_2O_3 composites fabricated by stir and compocasting processes," *Materials and Design*, vol. 34, pp. 106–111, 2012.

[4] K. B. Nie, X. J. Wang, X. S. Hu, L. Xu, K. Wu, and M. Y. Zheng, "Microstructure and mechanical properties of SiC nanoparticles reinforced magnesium matrix composites fabricated by ultrasonic vibration," *Materials Science and Engineering A*, vol. 528, no. 15, pp. 5278–5282, 2011.

[5] Q. B. Nguyen and M. Gupta, "Increasing significantly the failure strain and work of fracture of solidification processed AZ31B using nano-Al_2O_3 particulates," *Journal of Alloys and Compounds*, vol. 459, no. 1-2, pp. 244–250, 2008.

[6] Q. B. Nguyen and M. Gupta, "Enhancing compressive response of AZ31B magnesium alloy using alumina nanoparticulates," *Composites Science and Technology*, vol. 68, no. 10-11, pp. 2185–2192, 2008.

[7] Q. B. Nguyen, K. S. Tun, C. Y. H. Lim, W. L. E. Wong, and M. Gupta, "Influence of nano-alumina and sub-micron copper on mechanical properties of magnesium alloy AZ31," *Composites B: Engineering*, vol. 55, pp. 486–491, 2013.

[8] T. Zhong, K. P. Rao, Y. V. R. K. Prasad, F. Zhao, and M. Gupta, "Hot deformation mechanisms, microstructure and texture evolution in extruded AZ31 nano-alumina composite," *Materials Science and Engineering A*, vol. 589, pp. 41–49, 2014.

[9] X. Zhang, Q. Zhang, and H. Hu, "Tensile behaviour and microstructure of magnesium AM60-based hybrid composite containing Al_2O_3 fibres and particles," *Materials Science and Engineering A*, vol. 607, pp. 269–276, 2014.

[10] H. Cay, H. Xu, and Q. Li, "Mechanical behavior of porous magnesium/alumina composites with high strength and low density," *Materials Science and Engineering A*, vol. 574, pp. 137–142, 2013.

[11] Q. B. Nguyen, M. Gupta, and T. S. Srivatsan, "On the role of nano-alumina particulate reinforcements in enhancing the oxidation resistance of magnesium alloy AZ31B," *Materials Science and Engineering A*, vol. 500, no. 1-2, pp. 233–237, 2009.

[12] M. Habibnejad-Korayem, R. Mahmudi, H. M. Ghasemi, and W. J. Poole, "Tribological behavior of pure Mg and AZ31 magnesium alloy strengthened by Al_2O_3 nano-particles," *Wear*, vol. 268, no. 2-3, pp. 405–412, 2010.

[13] D. Lu, Y. Jiang, and R. Zhou, "Wear performance of nano-Al_2O_3 particles and CNTs reinforced magnesium matrix composites by friction stir processing," *Wear*, vol. 305, pp. 286–290, 2013.

[14] B. C. Pai, S. Ray, K. V. Prabhakar, and P. K. Rohatgi, "Fabrication of aluminium-alumina (magnesia) particulate composites in foundries using magnesium additions to the melts," *Materials Technology*, vol. 24, no. 1, pp. 31–44, 1976.

[15] K. Purazrang, P. Abachi, and K. U. Kainer, "Investigation of the mechanical behaviour of magnesium composites," *Composites*, vol. 25, no. 4, pp. 296–302, 1994.

[16] V. Massardier, P. Kerdelhué, P. Merle, and J. Besson, "Experimental study of the interaction of magnesium with the reinforcement in AlMgSi alloy/α-alumina platelet composites," *Materials Science and Engineering A*, vol. 191, no. 1-2, pp. 267–276, 1995.

[17] A. Contreras, E. Bedolla, and R. Pérez, "Interfacial phenomena in wettability of TiC by Al–Mg alloys," *Acta Materialia*, vol. 52, no. 4, pp. 985–994, 2004.

[18] A. D. McLeod and C. M. Gabryel, "Kinetics of the growth of spinel, $MgAl_2O_4$, on alumina particulate in aluminum alloys containing magnesium," *Metallurgical Transactions A*, vol. 23, no. 4, pp. 1279–1283, 1992.